Optical and Quantum Electronics **34:** 523–540, 2002.

Advanced boundary conditions for eigenmode expansion models

PETER BIENSTMAN* AND ROEL BAETS
Department of Information Technology, INTEC/IMEC, Ghent University, Sint-Pietersnieuwstraat 41, B-9000 Gent, Belgium
*(*author for correspondence: E-mail: peter.bienstman@rug.ac.be)*

Abstract. In order to realise the full potential of eigenmode expansion models, advanced boundary conditions are required that can absorb the radiation impinging on the walls of the discretisation volume. In this paper, we will discuss and compare a number of these boundary conditions, like perfectly matched layers (PMLs), open (leaky mode) boundary conditions and transparent boundary conditions (TBCs). We will also introduce the case of PMLs with infinite absorption and discuss its relation to leaky mode expansion, leading to a deeper insight into the physics of PML.

Key words: absorbing boundary conditions, eigenmode expansion, leaky modes, optical modelling, perfectly matched layers, transparent boundary conditions

1. Introduction

Vectorial eigenmode expansion models offer a number of advantages over other techniques like BPM (Scarmozzino *et al.* 2000) or FDTD (Taflove 1995). Eigenmode methods do not rely on spatial discretisation, but rather expand the field in terms of the eigenmodes of each longitudinally invariant layer. Because this generally introduces fewer unknowns than models based on spatial discretisation, eigenmode expansion techniques tend to be a lot faster (Bienstman and Baets 2001).

A potential problem however with eigenmode methods is that they require the structure under study to be enclosed in a metal discretisation volume, in order to get a discrete set of radiation modes. This can cause parasitic reflections, as the radiation emitted by a device being modelled cannot escape towards infinity, will reflect at the boundary and disturb the simulation results.

Therefore, in order to tap fully into the potential of these methods, it is vital to use boundary conditions that are more advanced than the traditional hard walls, which reflect all the incident radiation and thus disturb the simulation results. In this paper, we will discuss and compare some of these advanced boundary conditions.

A first boundary condition is the so-called perfectly matched layer (PML), which we will introduce as a lossless layer with a complex thickness. We will

also elucidate the relation between PML modes and the leaky modes of the corresponding open structure. Additionally, we will discuss the special case of a PML with infinite absorption.

A second class of boundary conditions is based on Hadley's transparent boundary condition (TBC), which is reflectionless for a given angle of incidence and does not violate the orthogonality of the eigenmodes.

In this paper, we will discuss and compare these boundary conditions and place them in a generalised framework.

2. Generalised dispersion relation

Before discussing the boundary conditions themselves, we will propose a generalised framework in which all these boundary conditions can be incorporated. To this end, we will derive the dispersion relation for a one-dimensional multi-slab waveguide between two generalised boundaries. We will concentrate on TE modes, the treatment of TM modes follows along similar lines.

Consider the situation depicted in Fig. 1. The actual waveguide structure will be treated as a black box, described by its transfer matrix relating the field at the top of layer 1 and the bottom of layer N:

$$\begin{bmatrix} F_N \\ B_N \end{bmatrix} = \begin{bmatrix} T_{11} & T_{12} \\ T_{21} & T_{22} \end{bmatrix} \begin{bmatrix} F_0 \\ B_0 \end{bmatrix} \tag{1}$$

Here F relates to the forward-propagating field in the $+x$ direction (i.e. away from the lower boundary), and B to the backward field propagating along $-x$. The lower boundary at $x = 0$ will impose a certain relation between forward and backward-propagating waves, e.g. described by a reflection coefficient $r_0 = F_0/B_0$. We can therefore write this boundary condition as

$$F_0 - r_0 B_0 = 0 \tag{2}$$

For the TE case, F and B are directly proportional to the electric field E_y (see e.g. Smith *et al.* 1991). A field distribution that satisfies this condition is trivially $F_0 = r_0$ and $B_0 = 1$. Using the transfer matrix formalism, we can propagate this field through the lower cladding, the black box and the upper cladding to arrive at the second boundary. At this wall, we impose a similar boundary condition:

$$r_N F_N - B_N = 0 \tag{3}$$

Note that in this case the reflected field propagates in the $-x$ direction. Expressing that the field at the upper boundary satisfies Equation (3), gives

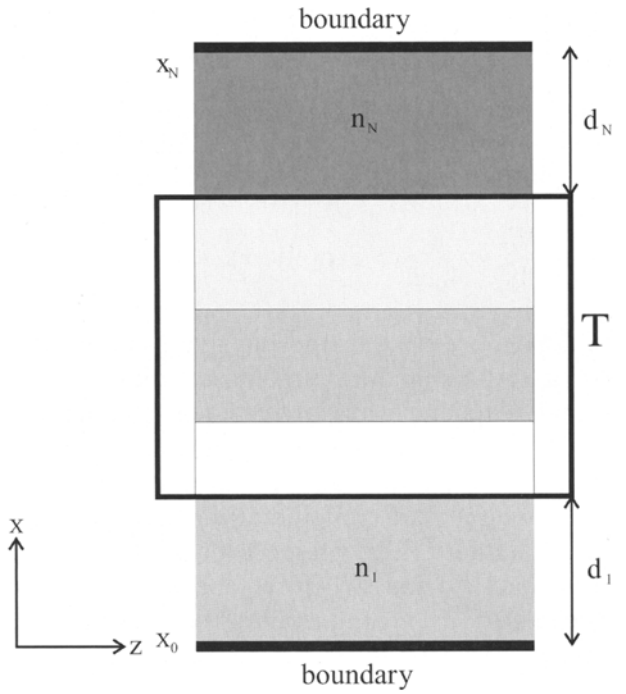

Fig. 1. Slab waveguide with general boundaries.

us the dispersion relation for a slab waveguide with generalised boundary conditions:

$$[r_N \exp(-\mathrm{j}d_N k_{x,N}) - \exp(+\mathrm{j}d_N k_{x,N})] \begin{bmatrix} T_{11} & T_{12} \\ T_{21} & T_{22} \end{bmatrix} \begin{bmatrix} r_0 \exp(-\mathrm{j}d_1 k_{x,1}) \\ \exp(+\mathrm{j}d_1 k_{x,1}) \end{bmatrix} = 0 \tag{4}$$

In the following sections, we will discuss different boundary conditions that can be expressed in this formalism. Note that in the most general case, the reflection coefficients r_0 and r_N can be functions of k_x. Stated otherwise, this means that the boundary conditions can depend on the incidence angle. We will concentrate on the boundary at $x = 0$, the other one obviously being completely analogous.

3. Hard walls

The most straightforward boundary conditions to use are perfect electric or magnetic conductors (PECs or PMCs). An electric wall imposes that the total tangential **E**-field vanishes at the boundary, which corresponds to the well-known Dirichlet boundary condition:

$$E_y(x=0) = F\exp(-\mathrm{j}k_x x) + B\exp(+\mathrm{j}k_x x) = 0 \tag{5}$$

Demanding that $F + B = 0$ amounts to choosing $r = -1$.

A magnetic wall imposes a zero tangential **H**-field. We can easily derive from Maxwell's equations that this means for TE modes that

$$H_z(x=0) = \frac{\mathrm{j}}{k_0 c\mu}\frac{\mathrm{d}E_y}{\mathrm{d}x} = \frac{k_x}{k_0 c\mu}(F\exp(-\mathrm{j}k_x x) - B\exp(+\mathrm{j}k_x x)) = 0 \tag{6}$$

So, for a PMC we choose $r = 1$. Imposing a vanishing derivative of E_y also means that this is a von Neumann boundary condition.

Both electric and magnetic walls are what is commonly referred to as 'hard' walls: they reflect all the incident power, because $|r| = 1$. This can be problematic, especially when we want to model structures with high radiation losses, i.e. structures that emit radiation that would otherwise propagate freely towards infinity. The presence of a PEC or a PMC wall will send this radiation back to the structure that we want to study, and this reflected power can seriously compromise the accuracy of the obtained results. Therefore, we need to introduce more advanced boundary conditions.

4. Perfectly matched layers

A PML is an artificial material that can absorb radiation without any parasitic reflections at its interface, regardless of wavelength, incidence angle or polarisation. The concept of PMLs can be introduced in a variety of ways, either using split fields (Bérenger 1994), anisotropic media (Sacks *et al.* 1995), or complex coordinate stretching (Chew and Weedon 1994). Here, we will opt for the formalism of complex coordinate stretching, because it allows us to reuse all the eigenmode formulas derived for the non-PML case without modification, simply by allowing the cladding thickness to assume complex values (Bienstman *et al.* 2001; Derudder *et al.* 2001).

4.1 COMPLEX COORDINATE STRETCHING

Consider the situation depicted in Fig. 2. A structure that we want to study is enclosed by a metal wall. This structure has an outer cladding layer with thickness d_0 and index n. Between the cladding and the wall, we insert the PML, a layer also with refractive index n, but with a complex thickness $d_{1,\mathrm{re}} - \mathrm{j}d_{1,\mathrm{im}}$. We want to prove in this section that a wave propagating in the

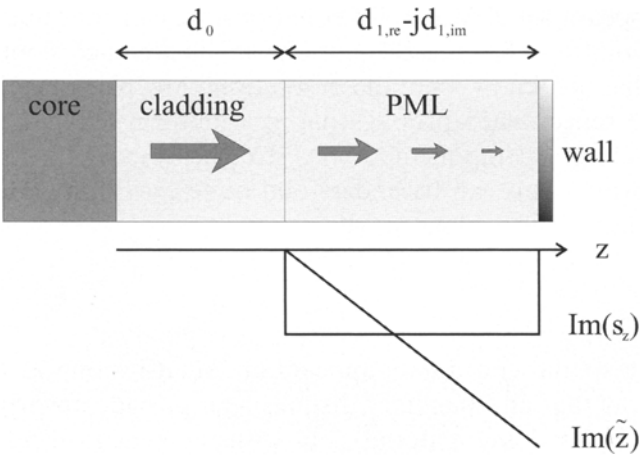

Fig. 2. Complex coordinate stretching.

cladding will be absorbed in the PML, without any reflections occurring at the cladding–PML interface. To this end, we first define a one-to-one mapping of the traditional z variable to a complex stretched $\tilde{z}$ variable (Chew *et al.* 1997):

$$\tilde{z} = \int_0^z s_z(z')\,\mathrm{d}z' \tag{7}$$

To make this more concrete, we have drawn in Fig. 2 the case were $\Re(s_z) = 1$ everywhere, and $\Im(s_z) = -a$ in the PML and zero everywhere else. This leads to $\tilde{z}$ being equal to z, except in the PML, where $\tilde{z}$ has a linearly increasing imaginary component (in absolute value). The use of an integral in Equation (7) assures that $\tilde{z}$ varies smoothly, even if s_z has discontinuities.

Now, we take Maxwell's equations and analytically extend them to the complex spatial domain. This means that the equations remain identical, but the coordinates are allowed to assume complex values.

$$\tilde{\nabla} \times \mathbf{E} = -\mathrm{j}\omega\mu\mathbf{H} \tag{8}$$

$$\tilde{\nabla} \times \mathbf{H} = \mathrm{j}\omega\varepsilon\mathbf{E} \tag{9}$$

The stretched nabla operator is

$$\tilde{\nabla} = \frac{\partial}{\partial x}\mathbf{u}_x + \frac{\partial}{\partial y}\mathbf{u}_y + \frac{\partial}{\partial \tilde{z}}\mathbf{u}_{\tilde{z}} \tag{10}$$

At this point we can understand why PML provides reflectionless absorption. From a purely formal point of view, the cladding combined with the PML is a uniform medium with refractive index n everywhere, but with stretched coordinates. Because coordinate stretching does not formally

change the appearance of Maxwell's equations, we can continue to use all the well-known solutions for these equations in unstretched coordinates. For uniform media, we know that these solutions are plane waves, which of course do not reflect when propagating in a uniform medium. At the same time, the imaginary component of the stretched $\tilde{z}$-coordinate absorbs the propagating wave. This can be understood quite easily e.g. when looking at the formula describing a plane wave:

$$\exp(-jknz) \tag{11}$$

Because the spatial coordinate appears on equal footing as the refractive index, it is clear that an imaginary distance can provide absorption just like an imaginary index (lossy material), but with the benefit of not introducing additional parasitic reflections, and this irrespective of wavelength, incidence angle or polarisation.

Finally, one can wonder if this rather ad hoc introduction of materials with complex thickness has any physical bearing whatsoever. In fact, as already mentioned previously, for the geometries we consider here a description in terms of complex coordinates is equivalent to the description of PML as an anisotropic material (Teixeira and Chew 1997). This material can of course be described completely by the traditional Maxwell's equations, without resorting to unphysical constructs like stretched coordinates. However, the mathematics of using anisotropic materials are much more involved, which is why we opted for using complex coordinates.

4.2. MODE STRUCTURE IN THE PRESENCE OF PML

Let us now first investigate the influence PML has on the propagation constants and field profiles of eigenmodes. The dispersion relation of a slab clad with PML is identical to the one without PML, except for the fact that the outer media have a complex thickness. The dispersion relation can therefore also be cast in the general formalism of Equation (4).

Fig. 3 shows the distribution of the TE modes in the n_{eff}-plane, for a GaAs waveguide ($n = 3.5$) with a thickness of 1 μm, surrounded on both sides by an air cladding with real thickness of 2 μm. The operating wavelength is 1.55 μm. Three figures are shown, for different imaginary thicknesses of the cladding (−0.2, −0.4 and −0.6 μm). A number of conclusions can be drawn from these pictures.

Let us first turn our attention to the guided modes, located on the real axis. Guided modes have exponentially decreasing tails, because they have an imaginary wavevector component in the direction perpendicular to the wall.

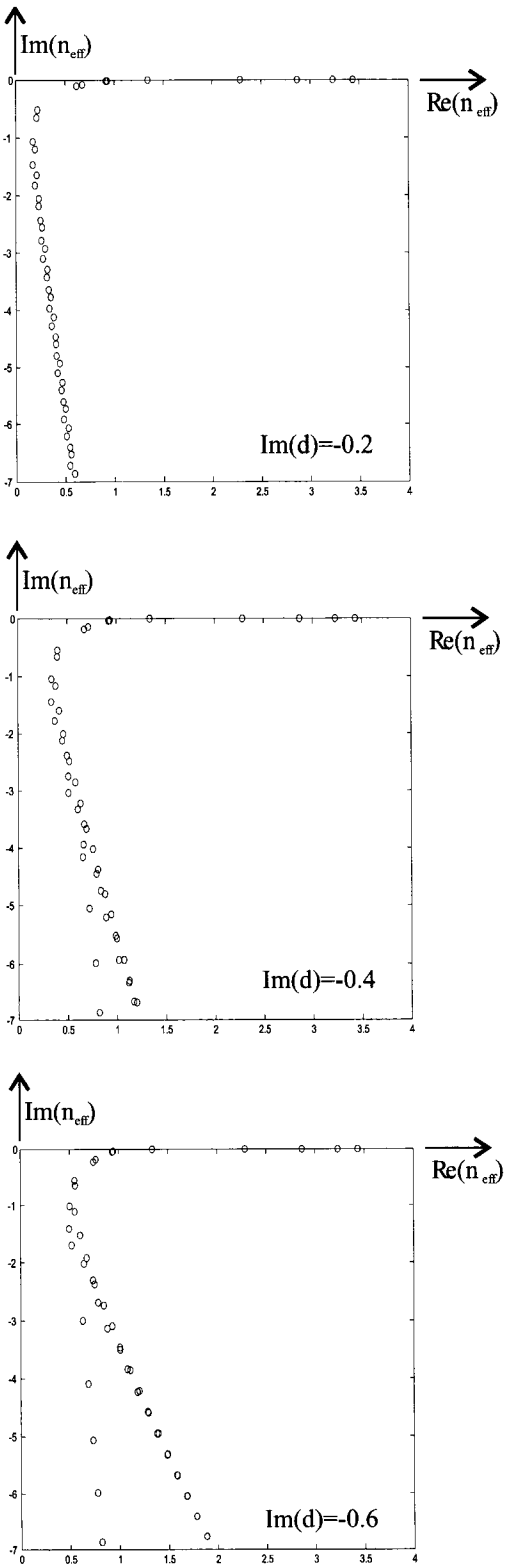

Fig. 3. Distribution of eigenmodes for different absorption levels in the PML.

If the cladding is thick enough, these tails will be negligible by the time they reach the PML, so they will not be influenced by it.

Radiation modes on the other hand are absorbed by the imaginary thickness, so that they are no longer located on the coordinate axes, but in the complex plane. In fact, when the absorption in the PML is strong enough, the modes clearly start to cluster in two groups: a first group, where the modes eventually converge to a final location for increasing PML absorption, and a second group, where the modes keep on moving further into the complex plane as the absorption increases. The profound reason for this behaviour will become clear in Section 5.

Let us now turn our attention to the field profiles of the radiation modes. Fig. 4 plots the absolute value of the **E**-field for a radiation mode with $n_{\text{eff}} = 0.416 - 1.600\text{j}$ in the case of an imaginary cladding thickness of $-0.4\,\mu\text{m}$. Fixing the total imaginary cladding thickness seems to leave us with the freedom of choosing the exact stretching profile to achieve this total thickness. Therefore, we plot two cases, both with a piecewise constant stretching profile s_z. In the first case, we choose the real thickness of the PML to be half of the cladding layer (1 μm), with the other half remaining unstretched. In the second case, we halve the PML thickness, but at the same time double its absorption. The field profiles in the central region are the same for both cases. In the cladding region, the field increases, but as soon as it enters the PML, it decreases exponentially to fall to zero at the metal wall.

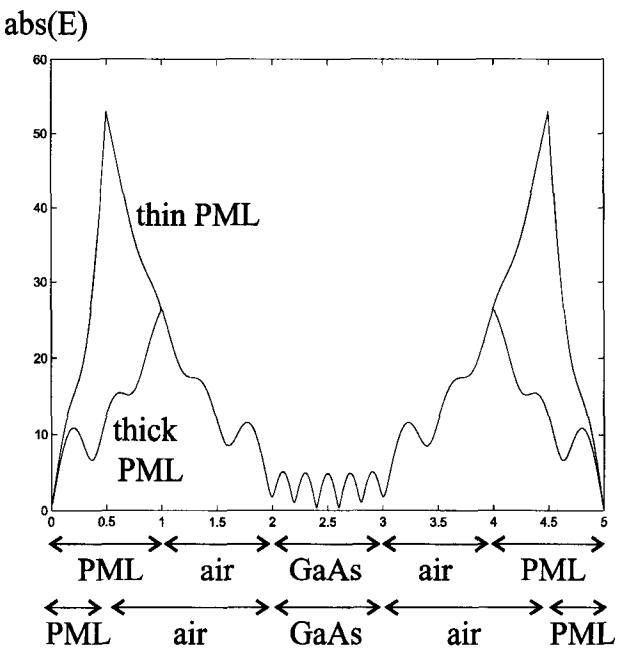

Fig. 4. Field profile of a radiation mode in the presence of PML.

For the thin PML, the field is allowed to increase further into the cladding, but this is exactly compensated by a stronger absorption inside the PML.

We want to stress that for the calculation of the dispersion relation, of the overlap integrals and of the scattering matrices, the exact stretching profile is totally irrelevant, because all the expressions there involve only the total complex thickness of the uniform medium formed by the combination of cladding and PML. This is a huge advantage compared to the use of PML in e.g. FDTD, where the stretching profile has to be carefully engineered in order to minimise reflections due to the spatial discretisation.

5. Leaky modes

Equation (4) also contains the dispersion relation for the open structure, i.e. without any walls. To retrieve this dispersion relation, we simply have to impose that there are no reflected waves in the cladding by putting the r coefficients equal to zero. It then follows immediately that $T_{22} = 0$, which is the required dispersion relation.

As is well-known, the dispersion relation of the open structure can have solutions in the complex plane (Oliner *et al.* 1981). These so-called leaky modes are unphysical, because they increase exponentially towards infinity in the transverse direction. They can be considered as guided modes below cut-off, because they will evolve into proper guided modes as the frequency increases. In Fig. 5, we plot the distribution of these modes in the n_{eff}-plane, for the same waveguide as in Fig. 3.

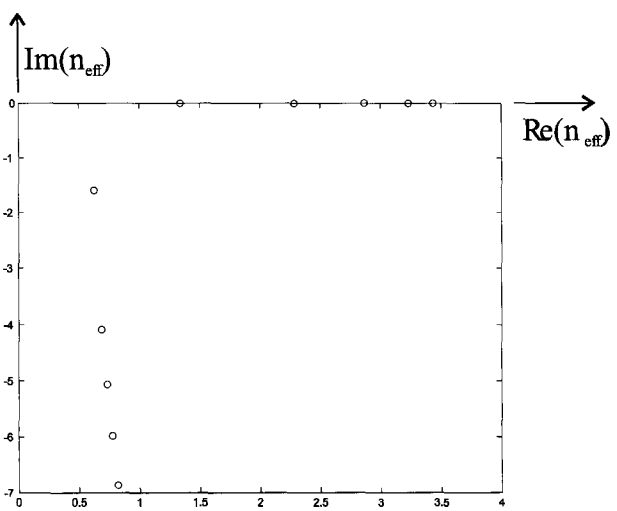

Fig. 5. Distribution of guided and leaky modes.

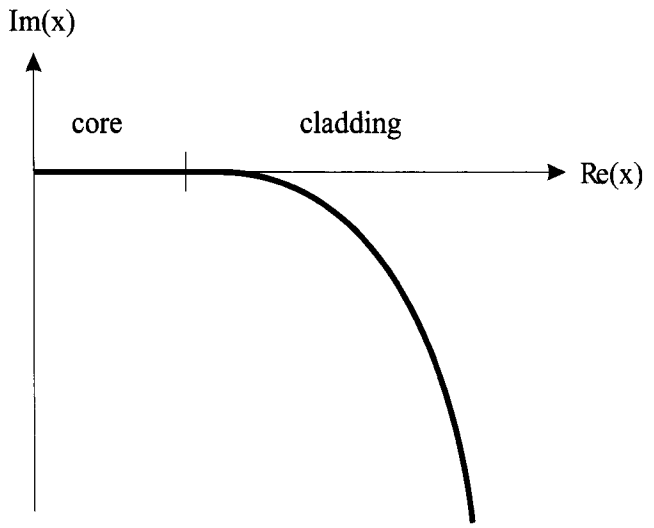

Fig. 6. Deformation of the integral path to calculate overlap integrals for leaky modes.

Because these modes form a discrete set, people have tried to use them in eigenmode expansion techniques. The hope here is that every leaky mode can represent a subset of the radiative continuum in open structures. When we want to apply the eigenmode expansion method to leaky modes, we quickly run into a problem concerning the overlap integrals. Indeed, these modes have infinite fields at infinity, meaning that the overlap integrals will diverge. A couple of techniques exist to deal with this issue (Lee *et al.* 1995), the most elegant of which is given by Sammut and Snyder (1976). The method presented there consists of deforming the integration path used to calculate the overlap and normalisation integrals. Normally, this path runs along the real x-axis, but it is deformed into the complex plane, as shown in Fig. 6. The analytical solution of the overlap integrals used in eigenmode expansion depends only on the beginning and end points of the interval. Therefore, the precise integration path is not important, only the end points are. If the damping provided by the complex coordinate at infinity outweighs the field increase in the cladding, then this contribution at infinity vanishes and the total overlap integral remains finite.

Although in some cases, most notably involving long waveguide sections with low index contrast, leaky mode expansion can be applied succesfully (Lee *et al.* 1995), this succes cannot be generalised to arbitrary structures. Moreover, it is possible to prove conclusively that the set of leaky modes is not complete (see e.g. Smith and Houde-Walter 1995). In view of this, it is quite ill-advised to rely solely on leaky mode expansion without any verification from another method.

5.1 RELATION TO PML

The path deformation used to normalise leaky modes is strongly reminiscent of the complex coordinate stretching PML technique. This suggests a closer relation between the two techniques, which we will try to uncover in this section.

Let us consider once again the general slab waveguide from Fig. 1 and its general dispersion relation Equation (4), in which we have factored out $\exp(+\mathrm{j}d_1k_{x,1})$ and $\exp(+\mathrm{j}d_Nk_{x,N})$. We will assume a very strong PML present in both claddings.

$$\left[r_N \exp(-2\mathrm{j}d_Nk_{x,N}) - 1\right] \begin{bmatrix} T_{11} & T_{12} \\ T_{21} & T_{22} \end{bmatrix} \begin{bmatrix} r_0 \exp(-2\mathrm{j}d_1k_{x,1}) \\ 1 \end{bmatrix} = 0 \tag{12}$$

If a certain mode is strongly attenuated in the top PML layer, then $d_Nk_{x,N}$ has a large negative imaginary component and $\exp(-2\mathrm{j}d_Nk_{x,N}) \ll 1$. Similarly, $\exp(-2\mathrm{j}d_0k_{x,0}) \ll 1$ for strong absorption in the bottom PML. We can now distinguish between four cases, depending whether a mode is strongly absorbed in both PML layers, only the top one, only the bottom one, or neither of them.

For the first set of modes, we assume strong absorption in both PMLs, such that most of the field is located in the central regions of the slab:

$$\begin{bmatrix} 0 & -1 \end{bmatrix} \begin{bmatrix} T_{11} & T_{12} \\ T_{21} & T_{22} \end{bmatrix} \begin{bmatrix} 0 \\ 1 \end{bmatrix} = 0 \tag{13}$$

This is satisfied when $T_{22} = 0$, which is nothing other than the dispersion relation of the open structure. Mathematically, this is also obvious, since infinite PML absorption [$\exp(-2\mathrm{j}dk) = 0$] has the same effect in Equation (13) as considering a truly open structure ($r = 0$). This is also what one expects from a physical point of view: as long as the absorption in the PML is high enough, no wave will make it back to the core after reflecting at the outer walls. Therefore, viewed from the core, a very strong PML cannot be distinguished from a truly open structure.

It is well-known what kind of modes are found with the dispersion relation of the open structure: on one hand the guided modes, but on the other hand also the unphysical leaky modes. This is precisely why some modes converge to a fixed location in Fig. 3: they converge to the leaky modes of the open structure for sufficiently large absorption in the PML.

For the second set of modes, we assume a field strongly damped in the PML at $x = 0$, but not so in the other PML layer. We now get for the dispersion relation

$$T_{12}r_N \exp(-2\mathrm{j}d_Nk_{x,N}) - T_{22} = 0 \tag{14}$$

which can be recast as

$$\exp(-\mathrm{j}d_N k_{x,N}) r_N \exp(-\mathrm{j}d_N k_{x,N}) \frac{T_{12}}{T_{22}} = 1 \tag{15}$$

This equation has a clear physical significance. The first factor describes propagation over a distance d_N in the PML, the second factor is the reflectivity at the wall, the third one describes the wave as it propagates from the wall back to the core, and the final term is the reflection of the core as seen from the top.[1] In other words, Equation (15) clearly imposes a round-trip gain of unity in the cavity formed by the top wall and the central slab.

A similar set of modes can be found that resonate in the bottom PML. Because the properties of these modes obviously depend more strongly on the PML than on the central core region, these modes are sometimes called Bérenger modes (Derudder *et al.* 2001). These Bérenger modes are the ones in Fig. 3 that move further into the complex plane as the PML absorption increases.

Finally, the case where the modes are neither absorbed in the top nor the bottom PML is purely academic, since it contradicts our initial assumption of a strongly absorbing PML.

6. PML with infinite absorption

In the previous section, we showed that for strong absorption in the PML, some modes converge to the leaky modes of the open structure. This result was first presented by Rogier and De Zutter (2001), but for the less general case of a microstrip substrate.

In the current paper, we want to take the argument one step further, and show that for infinite absorption in the PML, eigenmode expansion becomes completely equivalent to leaky mode expansion. In order to prove this, we need to elaborate on a couple of points.

First of all, for an infinitely strong PML, the modes from Equation (13) coincide exactly with the leaky modes of the open structure.

Secondly, the Bérenger modes vanish entirely if the absorption of the PML becomes infinite. This can be seen from Equation (15) and its corresponding physical picture that a resonator with infinite losses cannot sustain any modes. This also follows from the explicit formulas of the Bérenger modes presented by Rogier and De Zutter (unpublished data) for a microstrip substrate, where no non-trivial solutions remain for infinite absorption.

[1] This can be seen immediately from $\begin{bmatrix} r \\ 1 \end{bmatrix} = \begin{bmatrix} T_{11} & T_{12} \\ T_{21} & T_{22} \end{bmatrix} \begin{bmatrix} 0 \\ t \end{bmatrix}$.

Lastly, for infinitely absorbing PML, the calculation of overlap integrals proceeds in exactly the same way as in the case of leaky modes. Indeed, both use complex coordinate stretching to achieve absorption. For an infinitely strong PML, the contribution to the overlap integrals at the walls vanishes, just as the contribution at infinity in the case of leaky modes.

Together these arguments show that leaky mode expansion is nothing else than using a PML with infinite absorption. This sheds some more light on the physics behind each of these methods.

This also leads to some important observations with respect to the completeness of the set of eigenmodes in the presence of PML. If we assume an otherwise lossless structure, increasing the absorption in the PML leads from a set that is proven complete (for zero absorption) to a set that is proven incomplete (for infinite absorption). This suggests that while the set of modes in the presence of PML might not be mathematically complete, for all intents and purposes it is still close enough to complete if we restrict ourselves to moderate absorption. All the empirical evidence of the simulations we performed so far seems to show that this is indeed the case: for moderately strong absorption, using PML modes seems to be a very valid and practical approach. By moderate absorption, we mean a situation whereby the modes are still located relatively close to the coordinate axes, and where there is not yet a clear distinction between the Bérenger and the leaky branch.

Finally, it is worth noting that, just like leaky modes, PML modes exhibit an exponential field increase in the cladding before entering the absorbing region (see e.g. Fig. 4). This also indicates that the validity of the fields in the presence of PML seems to be limited to an area of the cladding immediately around the central region, just like leaky modes (Snyder and Love 1983).

7. Transparent boundary conditions

7.1. DERIVATION USING THE ORTHOGONALITY REQUIREMENTS

In this section, we will introduce transparent boundary conditions in a novel way, starting from the orthogonality requirements for eigenmodes. In order for eigenmodes to be orthogonal, it can be proven from the Lorentz reciprocity theorem that the following condition should hold at the boundary of the computational domain (see e.g. Lee 1986)

$$\int\int_{\delta S} (\mathbf{E}_1 \times \mathbf{H}_2 - \mathbf{E}_2 \times \mathbf{H}_1) \cdot \mathrm{d}\mathbf{S} = 0 \tag{16}$$

For the TE modes of the general slab waveguide and at the lower boundary at $x = 0$, this becomes

$$\int \left(E_{y,1}H_{z,2} - E_{y,2}H_{z,1}\right) \mathrm{d}z = 0 \tag{17}$$

At PEC or PMC walls, this is always fulfilled, since these boundaries impose the vanishing of the tangential electric field E_y or the tangential magnetic field H_z respectively. The presence of PML does not change this conclusion, since the PML is backed by a PEC or a PMC wall that imposes the same boundary conditions. Likewise, the orthogonality holds for the leaky modes as the special case of PML with infinite absorption.

Let us now decompose the fields at $x = 0$ in forward and backward propagating plane waves (see Equations (5) and (6)):

$$E_y = F + B \tag{18}$$

$$H_z = \frac{k_x}{k_0 c\mu}(F - B) \tag{19}$$

We can then write Equation (17) as

$$(F_1 + B_1)k_{x,2}(F_2 - B_2) - (F_2 + B_2)k_{x,1}(F_1 - B_1) = 0 \tag{20}$$

or as

$$k_{x,2}\frac{F_2 - B_2}{F_2 + B_2} = k_{x,1}\frac{F_1 - B_1}{F_1 + B_1} \tag{21}$$

This suggests using the following form of boundary condition, with $k_{x,0}$ an arbitrary constant:

$$k_x \frac{F - B}{F + B} = -k_{x,0} \tag{22}$$

Rewriting this in the canonical form $F - rB = 0$ (Equation (2)) gives us for the reflection coefficient

$$r = \frac{k_x - k_{x,0}}{k_x + k_{x,0}} \tag{23}$$

Note that this is a case where the reflection coefficient depends on the incident angle. The absolute value of r is always smaller than or equal to 1, and is identically zero for the angle corresponding to $k_x = k_{x,0}$.

Another way of looking at this boundary condition is to reformulate Equation (22) in terms of $E_y = F + B$ and its derivative $E_y' = -\mathrm{j}k_x(F - B)$:

$$-\mathrm{j}k_{x,0}E_y + E_y' = 0 \tag{24}$$

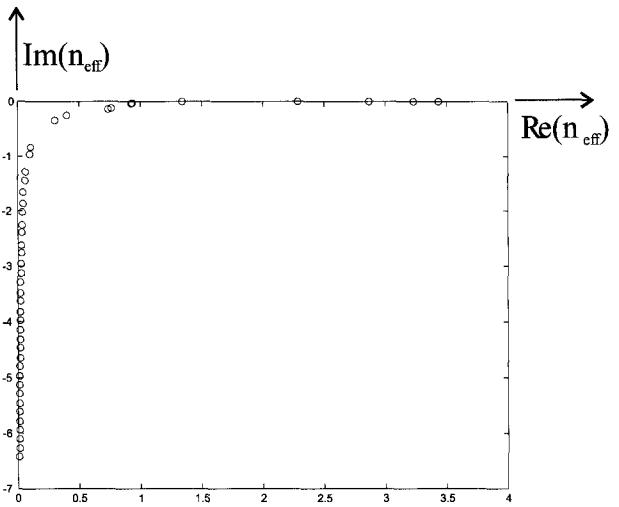

Fig. 7. Distribution of modes in the presence of a transparent boundary condition.

This is a mixed von Neumann–Dirichlet boundary condition with constant coefficients. For $k_x = k_{x,0}$ it is satisfied by $\exp(+jk_x x)$, which is a plane wave propagating downward from the core to the wall, without the presence of any reflected wave $\exp(-jk_x x)$.

This kind of boundary condition was presented by Hadley (1991), where it was called 'transparent boundary condition' (TBC) and applied to the beam propagation method. A similar boundary condition was already presented in a different context by Leontovich (1948). The TBC is also quite popular among MoL practitioners (Gerdes *et al.* 1992). Its use in eigenmode expansion methods has to our knowledge never been thoroughly studied, although the technique has been hinted at by Smith and Houde-Walter (1995).

Fig. 7 plots the distribution of eigenmodes for the slab waveguide from Fig. 3. The cladding is once again 2 μm thick, and the walls are TBCs with a $k_{x,0}$ corresponding to 45° incidence angle.

A striking feature of this figure is that the modes are located much closer to the coordinate axes, compared to e.g. PML and leaky modes.

7.2. EXAMPLE: LASER FACET

As an example, we take another benchmark problem that has been extensively studied in numerous papers in the literature (Ikegami 1972; Herzinger *et al.* 1993; Haes 1996). Its aim is to calculate the reflectivity of the cleaved end facet of a semiconductor laser, with the geometry of Fig. 8. The core has a width of 275 nm, and we consider the incidence of the fundamental TM mode at a wavelength of 860 nm, propagating horizontally to the facet on the

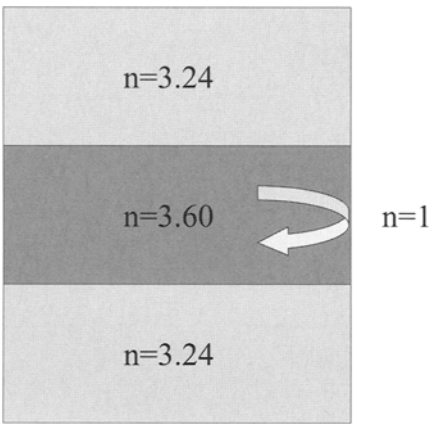

Fig. 8. Laser facet.

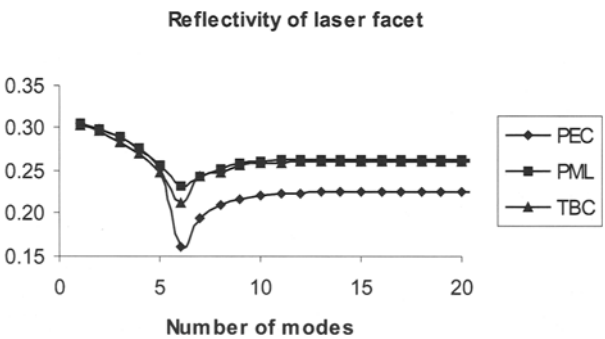

Fig. 9. Reflectivity of fundamental TM mode at laser facet.

right. An electric wall was used to exploit the symmetry along the propagation axis.

In Fig. 9, we plot the convergence of the reflectivity as a function of the number of modes, and this for different boundary conditions. We compare a PEC wall placed at 2 μm from the core, a PML layer with the same real thickness but with an imaginary thickness of -0.2 μm, and finally a TBC with zero reflection for 45° placed at the same real distance. All curves show a similar behaviour, i.e. they require about the same number of modes to converge to their final value. The reflectivity of the PML and TBC curve is in excellent agreement. The PEC curve however converges to a wrong value because of parasitic reflections. We can also obtain the correct result with a PEC, but only if we place the wall much further from the structure. This is of course at the expense of having to retain a much larger number of modes because of the larger computational domain. Advanced boundary conditions like PML and TBC therefore have an additional benefit next to their in-

creased accuracy: because the walls can be placed much closer to the structure under study, the calculation times can be drastically reduced (remember that these scale as N^3).

8. Conclusions

To conclude, we will compare the different boundary conditions presented in this paper. It is clear that hard walls are not very effective in modelling open space. Their only valid use is the exploiting of symmetries. Leaky mode expansion can give very good approximations with only a small number of modes, but unfortunately this method is only useful for a small number of structures. PML boundary conditions are very efficient, and have a much wider domain of applicability. They are reflectionless for any wavelength and provide moderate to strong absorption, making them very suited to model open space. Transparent boundary conditions exhibit zero reflectivities for a single angle and moderate to high reflectivities for other incidence angles. The fact that the zero-reflection angle has to be known in advance is sometimes a disadvantage.

In Fig. 10, we plot the power reflectivity of some of these boundary conditions: two PMLs with imaginary thickness of -0.2 and $-0.3\,\mu$m respectively backed by a PEC, and two TBCs with zero reflection at either 30° or 60°. The wavelength considered is 1 μm. The incident fields are plane waves that are propagative in the direction normal to the walls.

From Fig. 10, it can be seen that PMLs exhibit their lowest reflectivity for normal incidence. A larger imaginary thickness obviously means lower residual reflections. It is clearly visible that the TBCs have zero reflection for a single angle. If this zero-reflection angle moves to larger angles (i.e. towards grazing incidence), their reflectivity for the other angles increases. All the curves share the fact that their reflection approaches unity for grazing inci-

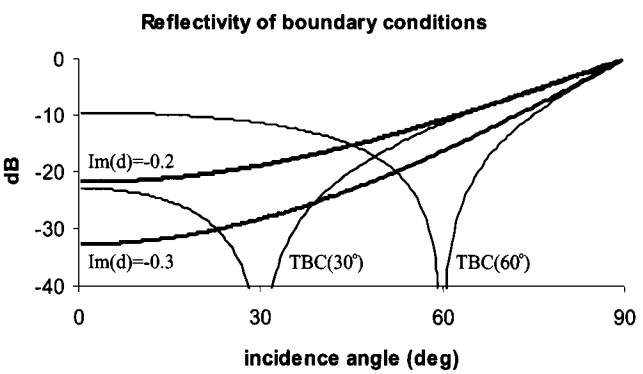

Fig. 10. Power reflectivity of different boundary conditions.

dence. This means that it will still be very difficult to absorb modes close to cut-off.

Finally, it has to be noted that nothing forbids us to combine both PML and TBC in a single boundary condition, in which case the total absorption in dB is the sum of the absorption of each of the individual boundary conditions. Such a combination is probably overkill in most situations, but could be useful for some simulations where extremely powerful absorbers are required.

Acknowledgements

Peter Bienstman acknowledges support from the Flemish National Fund for Scientific Research (FWO, Vlaanderen) through a doctoral fellowship. Parts of this work were also carried out in the context of the Belgian DWTC project IUAP IV 13.

References

Bérenger, J.-P. *J. Comput. Phys.* **114** 185, 1994.

Bienstman, P. and R. Baets. 2001, *Opt. Quant. Electron.* accepted for publication.

Bienstman, P., H. Derudder, R. Baets, F. Olyslager and D. De Zutter. *IEEE Trans. Microwave Theor. Tech.* **49** 349, 2001.

Chew, W., J. Jin and E. Michielssen. 'Complex coordinate stretching as a generalized absorbing boundary condition'. *Microwave Opt. Technol. Lett.* **15** 363, 1997.

Chew, W.C. and W.H. Weedon. 'A 3D perfectly matched medium from modified Maxwell's equations with stretched coordinates'. *Microwave Opt. Technol. Lett.* **7** 599, 1994.

Derudder, H., F. Olyslager, D. De Zutter and S. Van den Berghe. *IEEE Trans. Antennas Propagat.* **49** 185, 2001.

Gerdes, J., B. Lunitz and R. Pregla. *Electron. Lett.* **28** 1013, 1992.

Hadley, G.R. *Opt. Lett.* **16** 624, 1991.

Haes, J. Study of beam properties of laser diodes and design of integrated beam expansion structures. Ph.D. Thesis, Ghent University, 1996.

Herzinger, C., C. Lu, T. DeTemple and W. Chew. *IEEE J. Quantum Electron.* **29** 2273, 1993.

Ikegami, T. *IEEE J. Quantum Electron.* **8** 470, 1972.

Lee, D.L. Electromagnetic Principles of Integrated Optics, John Wiley and sons, New York, 1986.

Lee, S.-L., Y. Chung, L.A. Coldren and N. Dagli. *IEEE J. Quantum Electron.* **31** 1790, 1995.

Leontovich, M. Investigations of Radiowave Propagation, Part II. Printing house of the Russian Academy of Sciences, Moscow, 1948.

Oliner, A.A., S.-T. Peng, T.-I. Hsu and A. Sanchez. *IEEE Trans. Microwave Theor. Tech.* **29** 855, 1981.

Rogier, H. and D. De Zutter. *IEEE Trans. Microwave Theor. Tech.* **49** 712, 2001.

Sacks, Z., D. Kingsland, R. Lee and J. Lee. *IEEE Trans. Antennas Propagat.* **43** 1460, 1995.

Sammut, R. and A. Snyder. *Appl. Opt.* **15** 1040, 1976.

Scarmozzino, R., A. Gopinath, R. Pregla and S. Helfert. *IEEE J. Sel. Top. Quantum Electron.* **6** 150, 2000.

Smith, R. and S. Houde-Walter. *J. Opt. Soc. Am. A* **12** 715, 1995.

Smith, R., S. Houde-Walter and G. Forbes. *Opt. Lett.* **16** 1316, 1991.

Snyder, A. and J. Love. *Optical Waveguide Theory*. Chapman and Hall, London, 1983.

Taflove, A. Computational Electrodynamics, the Finite-Difference Time-Domain Method, Artech House, Norwood, MA, 1995.

Teixeira, F. and W. Chew. *Microwave Guided Wave Lett.* **7** 371, 1997.